JOURNAL OF APPLIED POLYMER SCIENCE VOL. 17, PP. 1227–1252 (1973)

Temperature Distribution in Semitransparent Plastic Sheets Exposed to Symmetric, Unsymmetric, and Pulsed Radiant Heating and Surface Cooling

R. C. PROGELHOF, *Newark College of Engineering, Newark, New Jersey,*
JAMES QUINTIERE, *National Bureau of Standards, Washington, D.C.*
and JAMES L. THRONE,* *American Standard, Inc.,*
New Brunswick, New Jersey

Synopsis

Solutions to the transient heat conduction equation subject to surface cooling and radiant heating are presented. The problem is associated with industrial methods of heating semitransparent plastic sheets for thermoform processing. Three cases are detailed: symmetric heating, unsymmetric heating, and pulsed, or "on-off," heating. The results demonstrate the effects of several parameters on the heating characteristics of the sheet. The method employed and solutions presented can serve to optimize thermoforming processes.

INTRODUCTION

In the plastics industry, the thermoforming operation is used to produce drawn profiles of plastic sheets for such applications as signs, skylights, and containers. The operation consists of an operator placing a plastic sheet between (or beneath) banks of infrared heaters, heating the sheet until he believes the sheet is soft and at a "forming" temperature, and then lowering the sheet onto a mold and applying vacuum to draw the sheet into its final form.

One of the more difficult and perplexing problems confronting thermoform processers is the determination of the temperature throughout the thickness of a sheet of transparent or semitransparent plastic as the sheet is being radiantly heated to a working condition. Much guesswork is required if the operator has had little experience in thermoforming a semitransparent sheet or is working with a new material. This is particularly true if the material is a laminate of semitransparent and opaque materials.

The purpose of this paper is the presentation of a set of analytical solutions to the transient heat conduction equation with boundary conditions that contain those factors that influence the radiant heating of a semi-

* Present address: Energetics Department, University of Wisconsin-Milwaukee, Milwaukee, Wisconsin 53201.

transparent plastic sheet. As illustration of the various solutions, the transient temperature distributions within a poly(methyl methacrylate) sheet are given.

PRIOR WORK

The principles of radiant heat transfer to semitransparent media reported in the literature have been developed primarily for solution to problems in the ceramic glass industry. A comprehensive review of the field, as well as prediction of the overall radiation characteristics of a semitransparent sheet, were given by Gardon in 1956.[1] In a subsequent paper,[2] Gardon applied these principles through numerical solution to the determination of the time–temperature history of a radiantly heated glass sheet. In 1965, Lich[3] presented a semianalytical solution for radiant heating of a semiinfinite body with physical properties that were independent of temperature and radiant wavelength. Perez and Baldo[4] and Fowle et al.[5] have since obtained numerical solutions to the set of equations that describe radiant heating of a sheet with variable thermal properties.

The only work specifically oriented toward plastics is that of Lunka.[6] He assumed complete surface absorption of the radiant energy by the plastic sheet. Progelhof et al.[8,9] have shown that certain plastics, such as acrylics used as an illustration by Lunka in his paper, do not absorb radiant energy solely on the surface, but have appreciable volume absorption. Lunka also determined the effect of pulsed, or "on-off," heating and recommended this method as a way of controlling sheet surface temperatures. Again, however, he assumed surface absorption of radiant energy.

THE POSED PROBLEM

As shown in Figure 1, we consider energy transport to a sheet of finite thickness, essentially infinite in directions perpendicular to the thickness. We assume that the sheet is exposed uniformly to radiant energy, that the physical properties of the sheet are temperature independent, that both surfaces of the sheet are smooth, and that polarization effects are negligible.

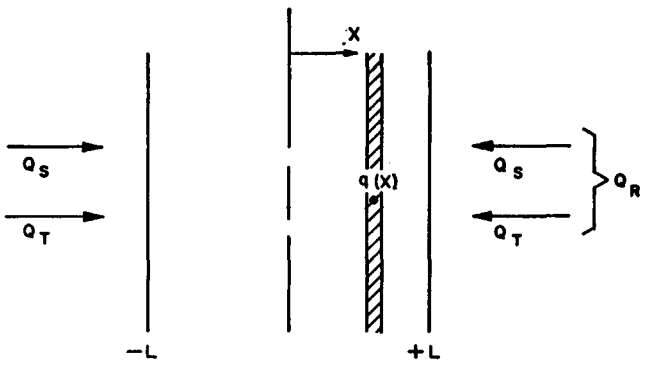

Fig. 1. Geometry for heating of a semitransparent sheet.

We assume further that the sheet contains no scattering centers and that reflectivity is independent of wavelength. This restriction is not inherent in the analysis but was made for ease in calculation. If a material exhibits large variations in reflectivity with wavelength, the distribution of energy within the sheet will be significantly affected. This can, however, be taken into account by simple modifications to this analysis. The internal and external reflectivities are assumed to be equal and determined from the index of refraction of the sheet by the Fresnel equation and Snell's law.[15] Thus, the temperature within the sheet is a function of the spatial coordinate, x, perpendicular to the sheet surface.

Energy is transported to and from the sheet in two ways: First, we assume that radiant energy sources, such as rod or filament heaters, are used and that the energy distribution on the surface of the sheet is uniform. The following heating conditions will be considered here: case 1, symmetrical heating; case 2, unsymmetrical heating with and without reflective presence of the environment behind the sheet; and case 3, pulsed, or on-off, heating.

Second, we assume that room-temperature air can be moved across the sheet surface. Using this model, we can gain some measure of the effect of the heat removal from the surface of the sheet.

Most radiation analyses assume relatively simple models for absorption into the materials.[7] The most familiar is the black body material, wherein all energy impinging on the surface of the body is absorbed. A second is a grey body material. Here, only a fraction of the energy is absorbed by the surface of the material, that fraction being independent of the wavelength of the incident radiant energy. Nearly all real materials are neither black nor grey bodies. Instead, the absorption of radiant energy is strongly wavelength dependent. In certain wavelength bands, the material may behave as if it were a black body, absorbing all incident radiant energy in that wavelength band. In other wavelength bands, the material may appear to be totally transparent to incident radiation. Radiation energy in this wavelength would pass through the material (regardless of the thickness of the material) without any loss of strength.

These are two approaches to analytical solution of complex radiation problems. The first develops differential heat balance into integro-differential equations. The analytical solutions to these equations are possible for relatively simple geometries and boundary conditions.[16] Computer solutions are required for more complex physical systems. The second approach described herein uses the "two flux" method. Although the method utilizes overall heat balances and is, therefore, approximate, the equations are more tractable, and more analytical solutions to pragmatic problems can be obtained. As a result, parametric studies can be carried out in greater detail, as we shall show.

The physical property of the material that is used to identify the degree of opacity or transparency is the absorption coefficient α, sometimes combined with the sheet thickness ($2L$) as the extinction thickness $2\alpha L$. The

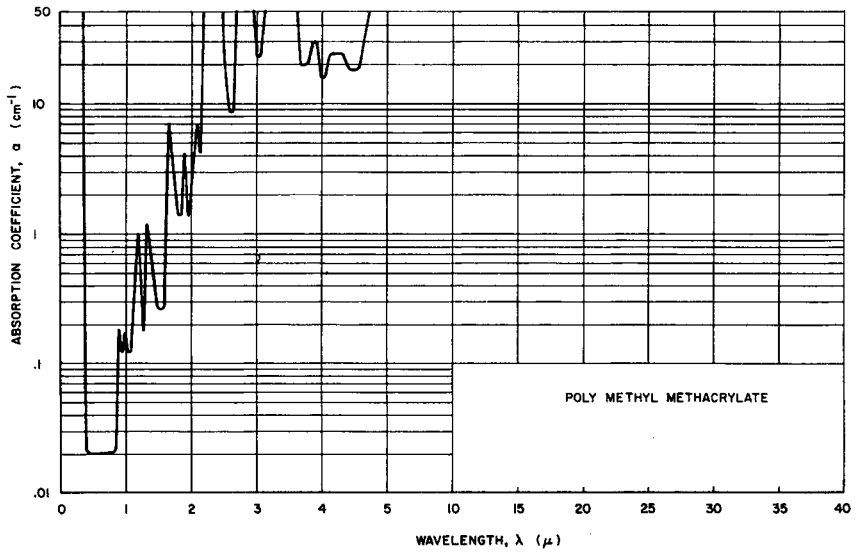

Fig. 2. Absorption spectrum for poly(methyl methacrylate).

smaller the value of the extinction thickness, the higher the transmittance of radiant energy through the sheet. If the value of the extinction thickness is infinite, the material is said to be opaque to incident radiant energy. Conversely, if the extinction thickness value is zero, the sheet is said to be transparent, regardless of its thickness.

Normally, for a given material the absorption coefficient is a highly irregular function of the wavelength. The absorption spectra for poly(methyl methacrylate) (Lucite) and poly(4-methylpentene-1) (TPX) are given as Figures 2 and 3, respectively.[8] In order to work with these curves in an analytical way, we approximate the curves with a series of step functions, following Gardon.[2] For each step, the absorption coefficient is assumed to be constant over a finite wavelength band. This method of approximation is demonstrated in Table I for Lucite and TPX.

For the regions where the absorption coefficient is neither infinite nor zero, the material is absorbing radiant energy throughout its volume. It is this fact that makes application of the basic principles of heat transfer complex and work such as that of Lunka[6] of questionable application when working with semitransparent sheet.

Mathematical Model

The temperature distribution within the sheet shown in Figure 1 is described by Fourier's equation with the generation term energy (representing volume radiant energy absorption) being treated as a lumped parameter that is only a function of the spatial coordinate[9] x:

$$\frac{\partial^2\theta}{\partial x^2} + \frac{q(x)}{k} = \frac{1}{\kappa}\frac{\partial\theta}{\partial t}. \tag{1}$$

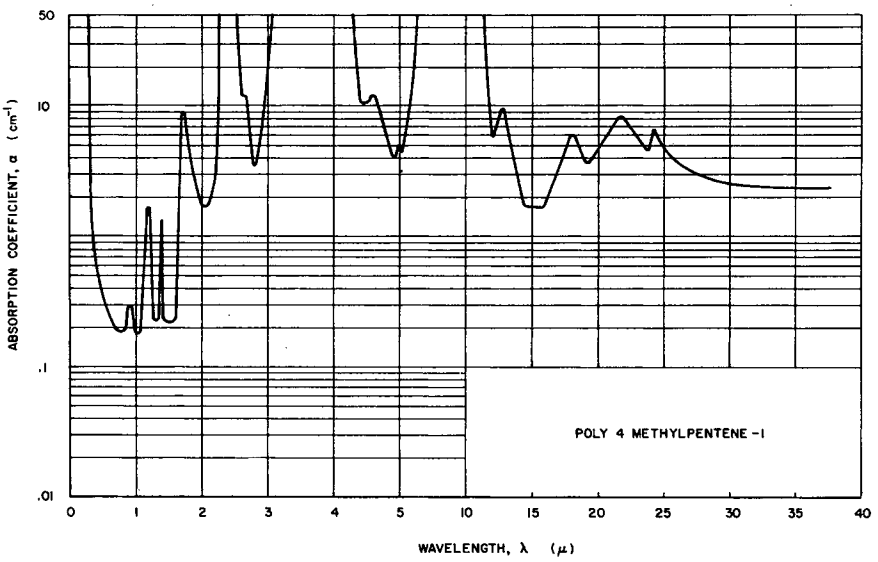

Fig. 3. Absorption spectrum for poly(4-methylpentene-1).

The boundary conditions that apply depend, of course, on the radiant heating condition. For case 1, symmetric heating,

$$\left.\frac{\partial\theta}{\partial x}\right|_{0,t} = 0 \tag{2a-1}$$

which assumes symmetry at the center of the sheet; and

$$-k\left.\frac{\partial\theta}{\partial x}\right|_{L,t} = -(1-\rho)Q_S + h\theta\Big|_{L,t} \tag{2b-1}$$

which is a heat balance at the surface of the sheet. In essence, eq. (2b) states that conduction within the sheet (the term on the left-hand side of the equation) must be balanced by that quantity of radiant energy absorbed on the surface (e.g., within the wavelength band where the absorption coefficient is infinite) and by the amount of heat added or removed by the moving air in contact with the sheet surface (the second term on the right-hand side of the equation). Here, of the energy Q_S that falls on the surface, ρQ_S is reflected (where ρ is the reflectivity from the sheet surface), and the remainder is absorbed. Further, h is the heat transfer coefficient, considered here to be the sum of convective and effective radiative coefficients. The remaining symbols are defined in the Nomenclature section.

For case 2, unsymmetric heating,

$$-k\left.\frac{\partial\theta}{\partial x}\right|_{L,t} = h\theta\Big|_{L,t} \tag{2a-2}$$

TABLE I
Step-Function Approximation to Absorption Spectrum

Wavelength λ, microns	Absorption coefficient α, cm^{-1}
Acrylic (Lucite)	
0 –0.4	∞
0.4 –0.9	0.02
0.9 –1.65	0.45
1.65–2.2	2.0
2.2 –∞	∞
Poly(4-methylpentene-1) (TPX)	
0 –0.3	∞
0.3 –1.6	0.25
1.6 –2.2	2.5
2.2 –2.7	∞
2.7 –2.9	5.0
2.9 –4.7	∞
4.7 –5.5	5.0
5.5 –12.0	∞
12.0 –13.5	6.0
13.5 –17.0	2.5
17.0–27.5	5.0
27.5–∞	2.5

which is a convective heat balance on the nonradiated side of the sheet, and

$$-k\left.\frac{\partial\theta}{\partial x}\right|_{-L,t} = -(1-\rho)Q_S + h\theta\Big|_{-L,t} \tag{2b-2}$$

which is a heat balance on the irradiated side of the sheet.

For case 3, pulsed heating, the boundary conditions for the symmetric case are

$$\left.\frac{\partial\theta}{\partial x}\right|_{0,t} = 0 \tag{2a-3}$$

and

$$-k\left.\frac{\partial\theta}{\partial x}\right|_{L,t} = -(1-\rho)Q_S S(t) + h\theta\Big|_{L,t} \tag{2b-3}$$

where

$$S(t) = \begin{cases} 1, & rt_p < t < rt_p + t_1 \\ 0, & rt_p + t_i < t < (r+1)t_p \end{cases} \qquad (r = 0, 1, 2, 3\ldots)$$

Here, t_p is the entire "on-off" period and t_1 is the "on" portion of the period. Also, Q_S should be interpreted here as the radiant flux during the "on" time, where $S(t)$ is dimensionless.

Similarly, for the unsymmetric pulsed case, Q_S is multiplied by S in eq. (2b-2).

The initial condition for eq. (1) is independent of the heating condition and is given as:

$$\theta|_{x,0} = 0. \tag{2c}$$

The heat generation term $q(x)$ can be obtained by generalizing Schuster's "two-flux" method.[10] For the unsymmetric case, the equation for $q(x)$ depends upon the physical geometry of the system, such as the presence of an "effective" external reflectivity ρ_s of the environment behind the sheet. If the environment is a black body absorber, $\rho_s = 0$. Whereas, if it is a perfect reflector, ρ_s is assumed to be unity. For a semitransparent sheet with a finite number of wavelength-independent absorption coefficients (N), the rate of energy generation within a sheet exposed symmetrically to radiation is

$$q_1(x) = \sum_{i=1}^{N} A_i \cosh \alpha_i x \tag{3-1}$$

where

$$A_i = \frac{2\alpha_i(1 - \rho)}{e^{\alpha_i L} - \rho e^{-\alpha_i L}} \int_{\lambda_i}^{\lambda_i + \Delta\lambda_i} Q_{R\lambda} d\lambda.$$

Here, the wavelength band λ_i to $\lambda_i + \Delta\lambda_i$ is the region where the absorption coefficient is finite. This is obtained in detail in Appendix A.

For the unsymmetrically heated sheet, this rate of energy absorption becomes

$$q_2(x) = \sum_{i=1}^{N} D_i[e^{\alpha_i(L-x)} + \{\rho + (1 - \rho)^2\rho_s\} e^{-\alpha_i(L-x)}] \tag{3-2}$$

where

$$D_i = \frac{\alpha_i(1 - \rho)}{e^{2\alpha_i L} - \rho\{\rho + (1 - \rho)^2\rho_s\} e^{-2\alpha_i L}} \int_{\lambda_i}^{\lambda_i + \Delta\lambda_i} Q_{R\lambda} d\lambda.$$

This expression is also obtained in detail in Appendix A.

For case 3, pulsed heating, note that $q_3(x)$ is piecewise-continuous in time since Q_R is finite for $rt_p < t < rt_p + t_1$ and zero for $rt_p + t_1 < t < (r + 1)t_p$. The energy generation term $q_3(x)$ for case 3 is given by eqs. (3-1) and (3-2), with the above-noted restriction.

In order to present the solution in a more conventional form, the following dimensionless variables and parameters are used:

$$\tau = \kappa t/L^2, \qquad \text{a dimensionless time (Fourier no.)}$$

$$\xi = x/L, \qquad \text{a dimensionless thickness}$$

$$\phi = \frac{T - T_0}{(L/k)(1 - \rho) \int_0^{\infty} Q_{R\lambda} d\lambda}, \qquad \text{a dimensionless temperature}$$

$$F_i = \frac{\int_{\lambda_i}^{\lambda_i+\Delta\lambda_i} Q_{R\lambda} d\lambda}{Q_R},$$ the fraction of radiant energy falling on the sheet between the wavelengths $\lambda_i + \lambda_i + \Delta\lambda_i$

$$\Omega_i = \alpha_i L,$$ a radiant extinction length

$$\bar{\rho} = \rho + (1 - \rho)^2 \rho_s,$$ a reflectivity parameter

$$\eta_{i1} = \frac{2\Omega_i}{(e^{\Omega i} - \rho e^{-\Omega_i})},$$ a radiation parameter for symmetric cases

$$\eta_{i2} = \frac{\Omega_i}{e^{2\Omega i} - \rho\bar{\rho}e^{-2\Omega_i}},$$ a radiation parameter for unsymmetric case

$B_i = hL/k,$ the ratio of resistance of the sheet to conduction and to convection (the Biot no.)

The complete solutions to eq. (1), subject to the boundary conditions of each of the three cases, are presented in detail in Appendix B. Each solution is comprised of two parts, a transient part and a steady-state component. In case 2, unsymmetric heating, the presence of a reflective second surface complicates the solution and the value of the external reflectivity ρ_s becomes important. In case 3, pulsed heating, the piecewise continuous boundary condition requires use of the Duhamel theorem[11] to affect a solution. It can be shown, however, that if T_1 (the dimensionless time for which the heaters are "on") is allowed to be T (the dimensionless period), the solution reduces to the case 1 or case 2 solution, accordingly. Further, if T_1 is set to zero, the solution becomes the solution of a simple, transient heat conduction equation.[7]

Implication of Solution Results

To determine what effect the various parameters have on the temperature distribution in the sheet, a series of calculations were made for the poly-(methyl methacrylate) sheet. The sheet is assumed to be 1 cm thick ($L = 0.5$ cm) and to have the following physical properties[12] at 70°F:

$$\kappa = 11.7 \times 10^{-4} \text{ cm}^2/\text{sec}$$

$$k = 4.83 \times 10^{-4} \text{ cal/cm sec °K}$$

The absorption coefficient for the acrylic was idealized as given in Table I. The nondimensional time parameter τ is related to the actual time by:

$$\tau = \kappa t/L^2 = 0.2808t$$

where t is in minutes. Thus, τ equal to 1.0 corresponds to a heating time of 3.56 min. The heat transfer coefficient h was assumed to be 1, 5, or 20 Btu/ft² hr °F.

Figures 4 and 5 show comparisons of the nondimensional temperature distributions for symmetric heating in the acrylic sheet (case 1) as functions of the temperature of the primary radiating source for constant Biot

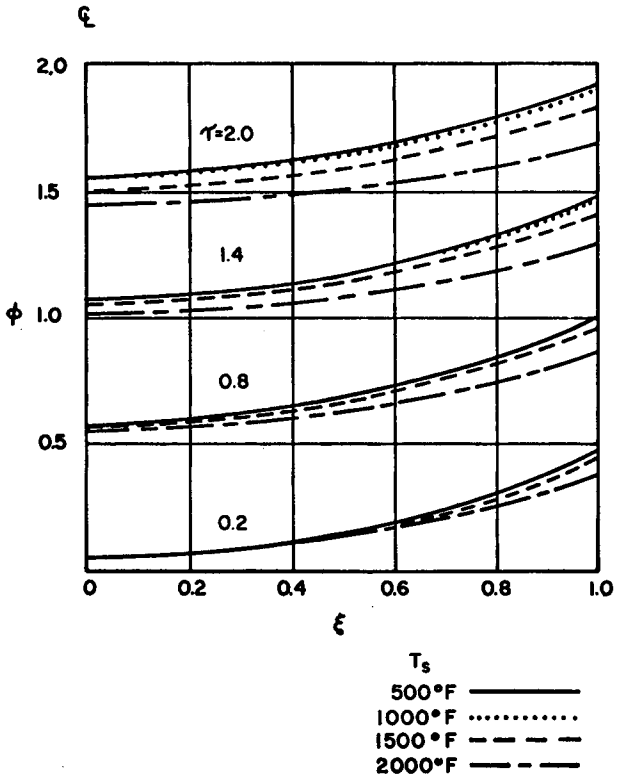

Fig. 4. Temperature–time profile for symmetric heating. Source temperature as parameter, $Bi = 0.1406$.

numbers. Without a loss in generality, the source was considered to have a black-body radiant distribution. A cross plot of the data for constant source temperature of 1500°F for varying amounts of surface cooling is given as Figure 6. From these figures it is evident that source temperature and convective film coefficient have marked effects on the uniformity of the temperature profiles within the sheets.

These plots do not indicate the relative magnitudes of the effects. To determine the relative degree of temperature uniformity within the sheet, another dimensionless parameter, referred to as the "evenness index," EI, is introduced. The evenness index is defined in terms of the material temperature, which in turn can be related to the nondimensional temperature:

$$EI = \frac{T_{max} - T_{min}}{T_{max} - T_0} = \frac{\phi_{max} - \phi_{min}}{\phi_{max}}.$$

To determine the effect of source temperature using the evenness index, the data of Figure 5 are replotted. These results are shown in Figure 7. The trend to more uniform heating with increasing surface temperature

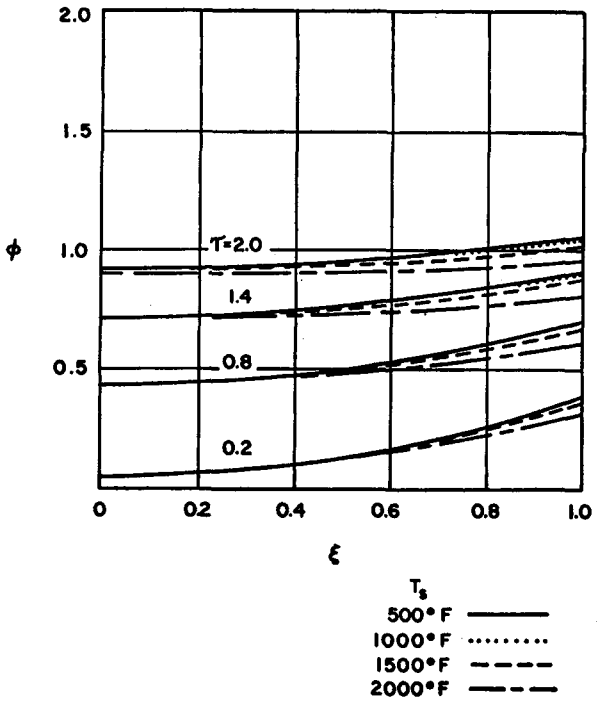

Fig. 5. Temperature–time profile for symmetric heating. Source temperature as parameter, $Bi = 0.703$.

as indicated in Figures 4 and 5 is clearly seen. This result can be explained by the general shape of the spectral absorption curve for acrylic. At low temperatures, the impinging radiant energy is absorbed solely at the surface of the sheet. As the source temperature is raised, a greater portion of the total incident radiation is absorbed within the sheet rather than at its surface. For example, if the source temperature is 500°F, less than 1% of the radiant energy emitted has a wavelength in that portion of the spectrum where volume absorption can take place. For a 2000°F source, however, 28% of the radiant energy is in the volume absorption portion of the spectrum.

To determine the effect of surface cooling, the data of Figures 4 and 5, as well as data for Biot number = 2.812, are replotted in terms of the evenness index. These results are shown in Figure 8. The utility of the evenness index is now apparent. The data of Figures 4 and 5 indicate that an increasing Biot number (e.g., greater surface cooling) produces a more uniform temperature distribution within the sheet. However, from Figure 8, it is now apparent that increased surface cooling has a more complicated effect on the temperature distribution. There is a specific time at which the sheet attains uniform temperature. For times greater than this, the temperature of the interior of the sheet becomes greater than the surface temperature; thus, the *EI* increases. This phenomenon can be explained

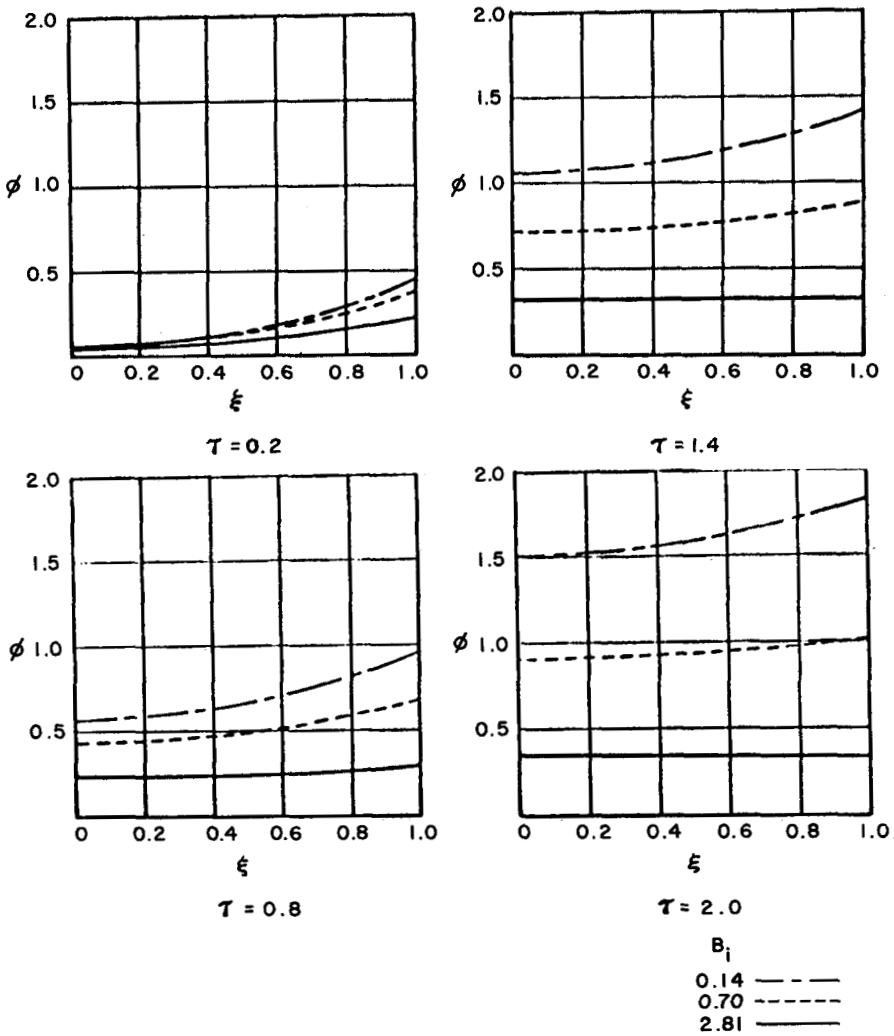

Fig. 6. Temperature–time profiles for symmetric heating. Biot number as parameter, $T_S = 1500°F$.

in the following manner: As the surface cooling is increased, a greater portion of the radiant energy absorbed at the surface is transferred to the surrounding medium. Thus, the net energy transferred into the sheet at the surface is smaller. Since changing the rate of surface cooling has no effect on the amount of energy absorbed within the sheet, the relative ratio of energy absorbed on the surface to volume absorption within the sheet is smaller. As the surface temperature of the sheet increases, the net flow of energy at the surface will approach zero. This leads to a uniform temperature profile. However, the rate of absorbed energy within the sheet is constant; thus the internal temperature still increases, resulting in an increasing EI.

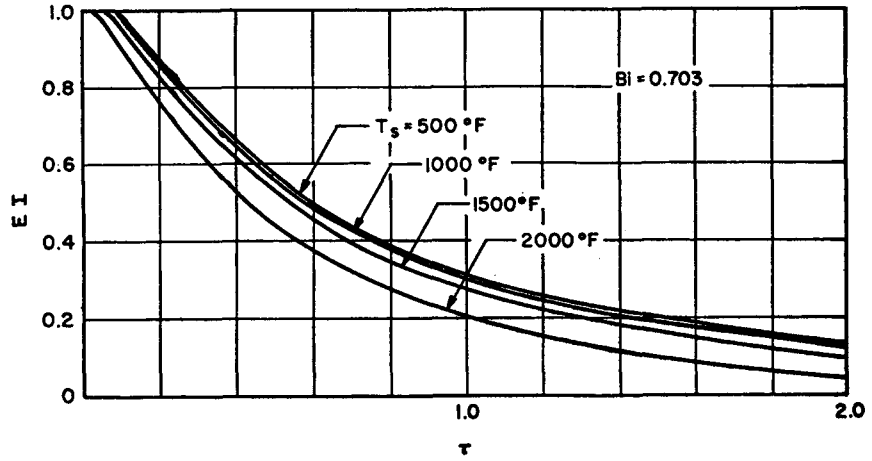

Fig. 7. Evenness index for symmetric heating. Source temperature as parameter.

Substantiation of these temperature profiles have not been carried out in detail to date. However, one corporation has found that incandescent sources (above 4000°K) heat semitransparent sheet faster and more uniformly than do rod heater sources.[17,18] In another area, Sliepcevich and co-workers[19] have found that time to achieve ignition with clear Plexiglas increases exponentially with increasing radiation source temperature at constant incident radiant flux, and they thus conclude that a solar furnace would probably not ignite their specimen of 1.27-cm thickness. We conclude from this that transmittance and volume absorptance have combined to limit volumetric material temperature.

An added effect, the presence of the environment, is shown in Figures 9 and 10 where, for case 2, unsymmetric heating, the nondimensional temperature distribution in the acrylic sheet is given as a function of "effec-

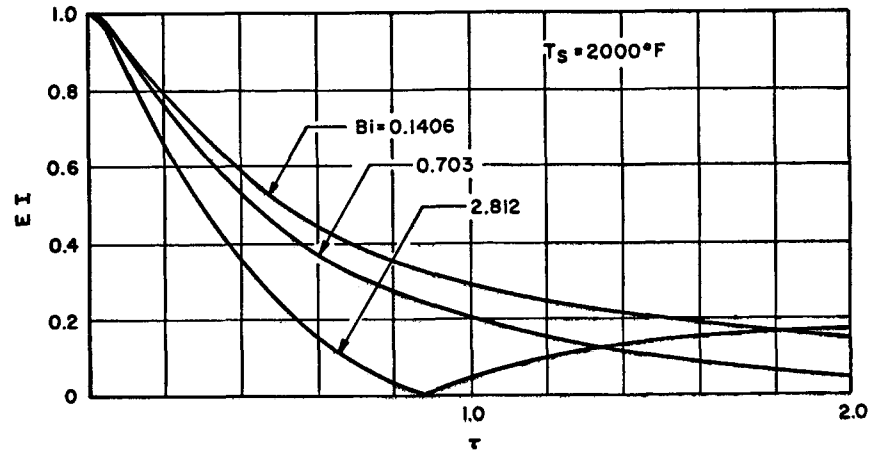

Fig. 8. Evenness index for symmetric heating. Biot number as parameter.

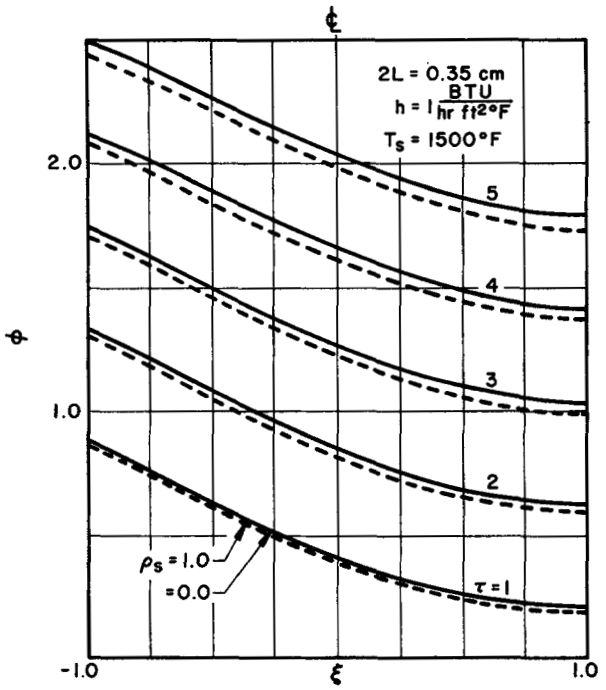

Fig. 9. Temperature–time profile for unsymmetric heating. External reflectivity ρ_s as parameter. Sheet thickness, $2L = 0.35$ cm.

tive" mold reflectivity and sheet thickness for constant source temperature, convective film, and sheet thickness coefficient. A cross plot of the data, for constant source temperature, heat transfer coefficient, and external reflectivity for varying sheet thickness is shown in Figure 11. From these figures it is evident that for acrylic, the "effective" mold reflectivity has relatively little effect, whereas sheet thickness is important. However, for a highly transparent material, such as TPX or polystyrene, a greater portion of the irradiant energy passes through the sheet, is reflected, and passes through the sheet again. The slightly different shape ($\tau = 5.0$) of the three curves is due to the relative magnitudes of sheet thickness to absorption coefficient α.

To determine the effect of symmetry, the temperature distribution in the acrylic sheet for symmetric and unsymmetric irradiation is given as Figure 12. Here, the total amount of radiant energy is the same in both cases. In Figure 13, the effectiveness of each heating rate is given using the evenness index EI as a basis.

As mentioned earlier, on-off heating during thermoforming of plastic sheets is a recommended practice.[6] For illustration, the total on-off period was assumed to be either 12 or 48 sec ($T = 0.05$ or 0.20). These values were motivated by Lunka's paper[6] in which he used a total period of 15 sec. With heaters on for 50% of the period for a source temperature of

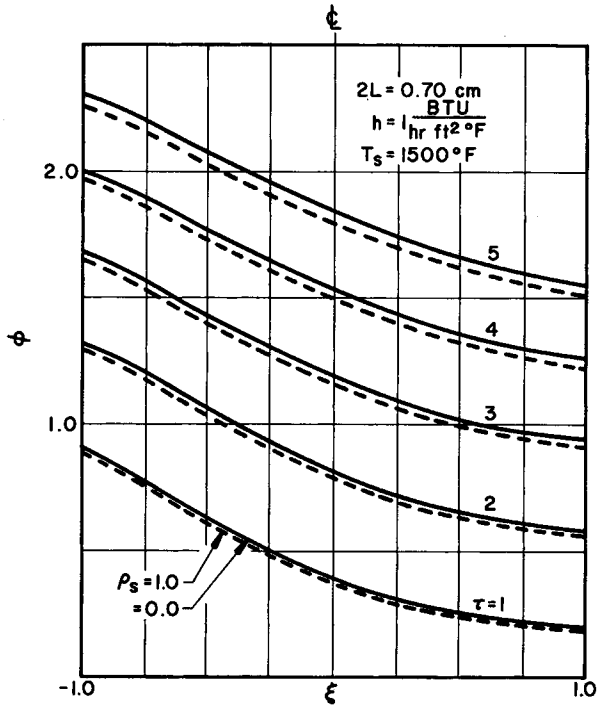

Fig. 10. Temperature–time profile for unsymmetric heating. External reflectivity ρ_s as parameter. Sheet thickness, $2L = 0.70$ cm.

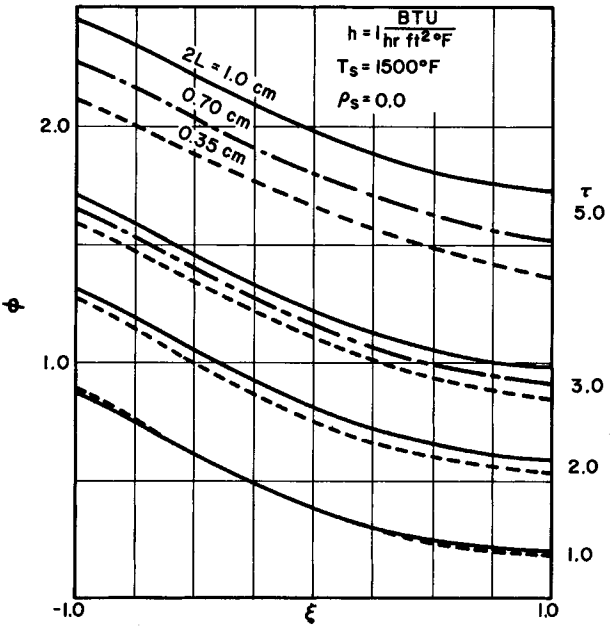

Fig. 11. Temperature–time profile for unsymmetric heating. Sheet thickness as parameter.

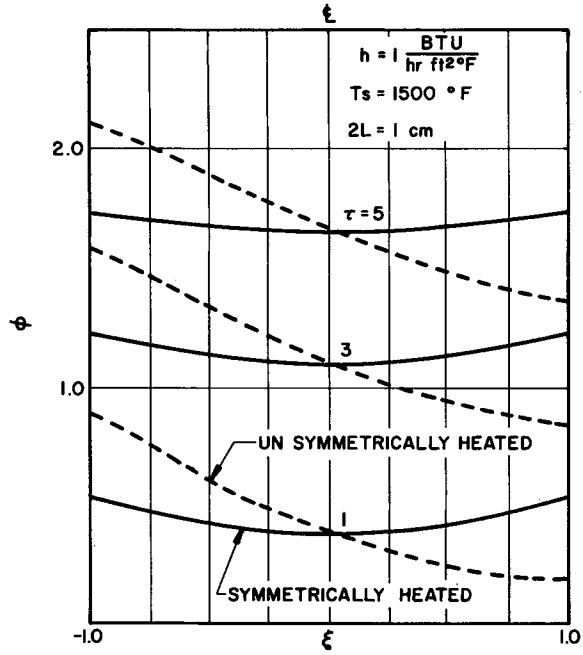

Fig. 12. Comparison of symmetric and unsymmetric temperature–time profiles.

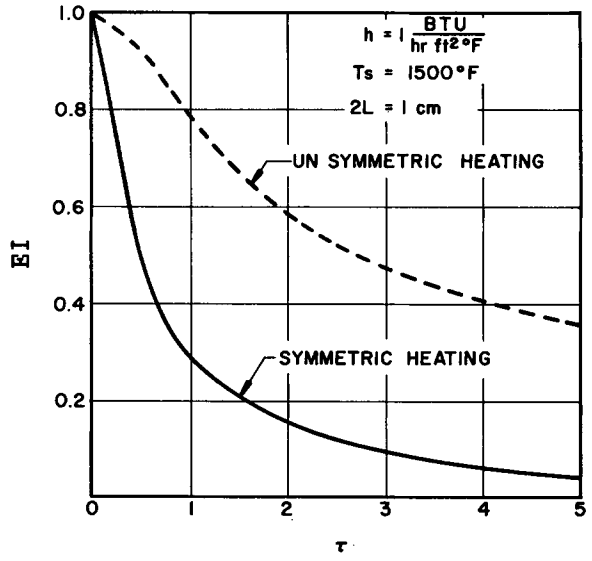

Fig. 13. Comparison of evenness indices for symmetric and unsymmetric heating.

1500°F, the corresponding temperature and evenness index are shown in Figure 14 as functions of dimensionless time for the two values of T. Note that the maximum temperature is relatively unaffected by the period, as might be intuitively expected. However, the maximum-to-minimum

temperature difference is markedly decreased by increasing the period. By comparing Figures 13 and 14, it is immediately obvious that unsymmetric heating leads to the most uneven form of heating and long-period pulsed heating to the most uniform form of heating. This is, again, intuitively expected.

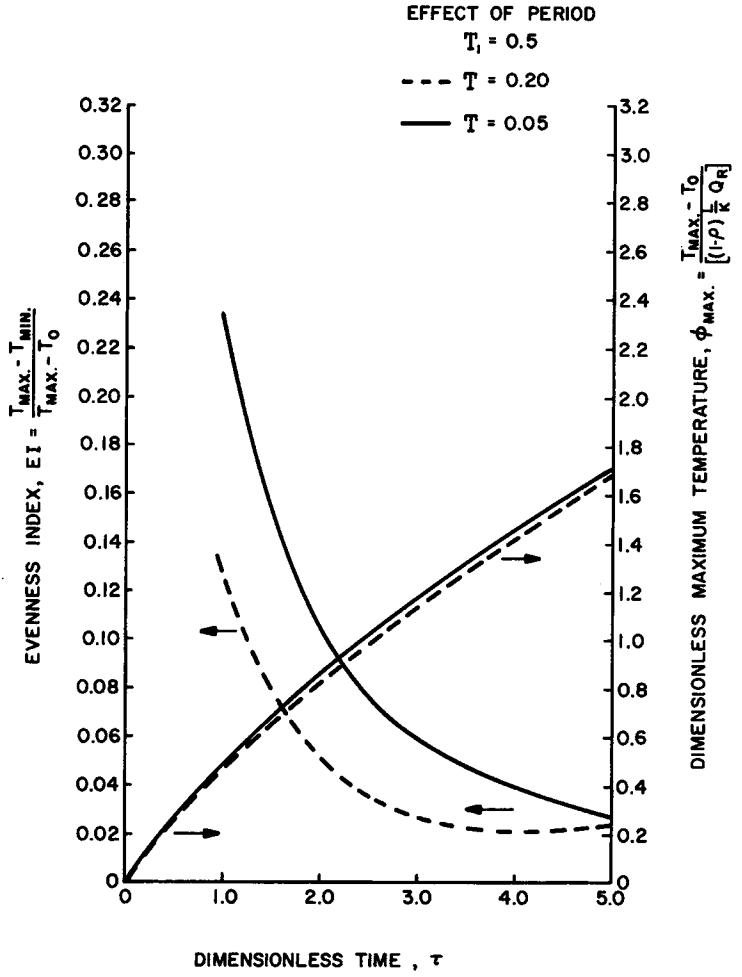

Fig. 14. Temperature and evenness index for pulsed symmetric heating. Total period as parameter. "On" period 50% of total period.

The effect of heating ratio on maximum temperature and EI is shown in Figure 15. Here, the "on" period is shown as 25%, 75% and 100% of the total period, $T = 0.05$. The curves labeled "$(T_1/T) = 1.0$" are identical to the Case 1 curves of Figures 12 and 13. Note here the dramatic (and, again, expected) decrease in temperature with decreasing extent of "on" period.

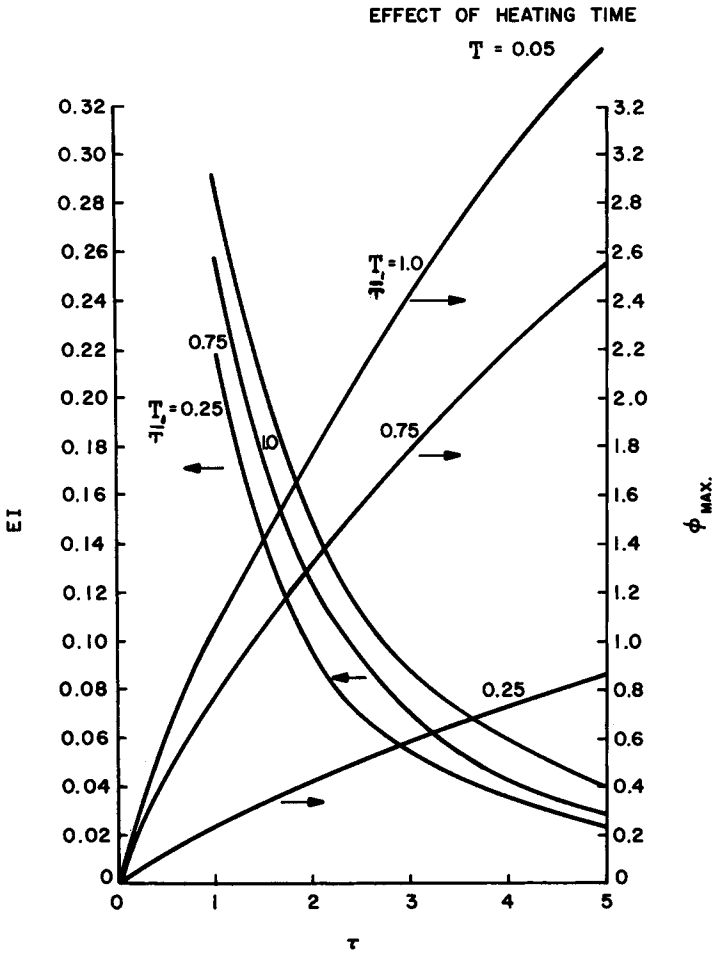

Fig. 15. Temperature and evenness index for pulsed symmetric heating. "On" period as parameter.

Note the very uniform temperature profiles through the sheet in Figure 16. Comparison of these curves with the case 1 temperature profiles of Figures 4 and 5 give theoretical credance to the pragmatic reasons for pulsed heating of temperature-sensitive sheets.

The solution to the unsymmetric heating problem (case 2) can be used with the Duhamel theorem to generate solutions to the unsymmetric heating problem with pulsed heating. As a representative example of such a solution, Figure 17 shows a comparison of temperature profiles for symmetric and unsymmetric pulsed heating for a total period of approximately 4 min and a 50% "on" portion. Comparing this figure with Figure 12, which gives temperature profiles for continuous (100%) "on" portion of the total period, it is again obvious that significant flattening of the temperature profile is accomplished by pulsed heating.

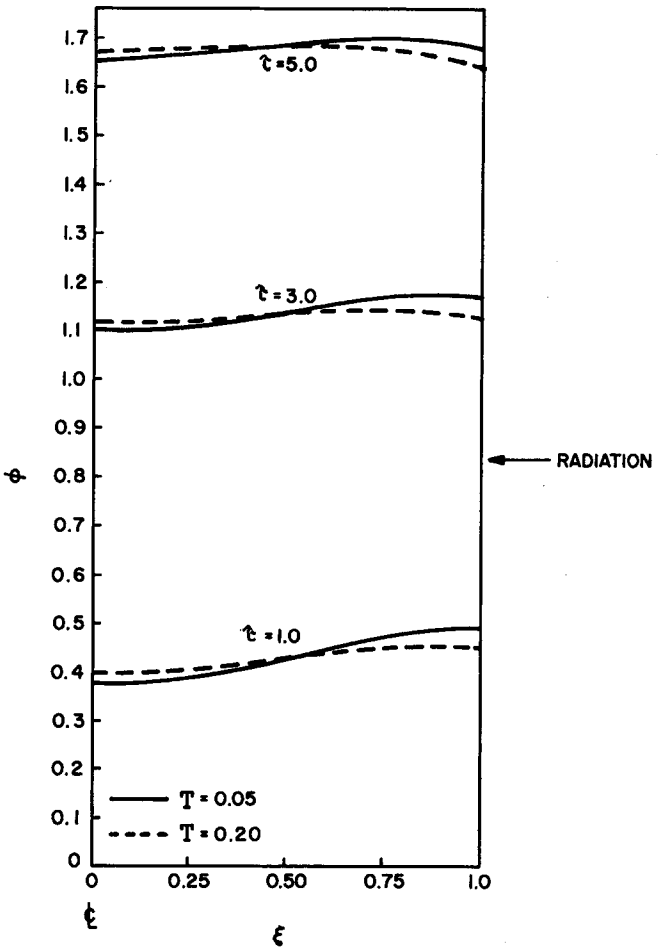

Fig. 16. Temperature–time profile for pulsed symmetric heating. Total period as parameter.

CONCLUSIONS

An extensive analysis of radiant heat transfer to a semitransparent sheet has been described in detail. Three cases have been analyzed: symmetric heating, unsymmetric heating, and pulsed, or "on-off," heating.

Poly(methyl methacrylate) properties were used for illustration of the solutions, which are presented in dimensionless form. Among the important results of this analysis were:

1. The spectral curve for the plastic has a strong influence on the temperature of the radiant source.

2. Increasing surface cooling (for symmetric heating) increases the temperature uniformity through the sheet but decreases the overall rate of heating, as is expected.

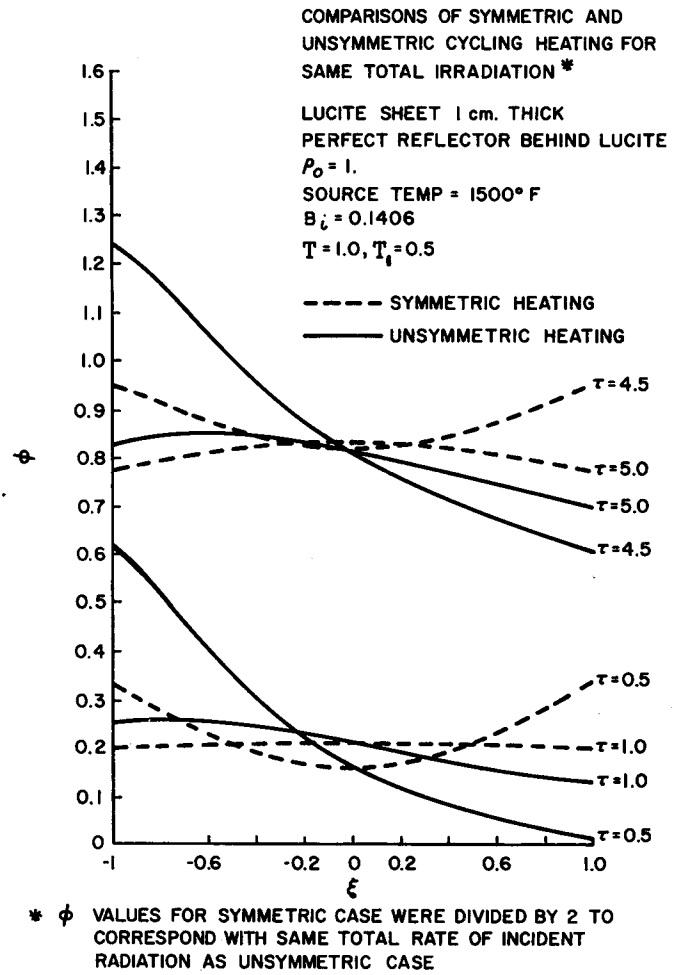

Fig. 17. Comparison of temperature–time profiles for pulsed symmetric and unsymmetric heating.

3. Volumetric radiant absorption is exponential with thickness, and thus thick sheets heat much slower than do thin sheets.

4. The presence of an absorptive or reflective wall behind an unsymmetrically heated acrylic sheet has little effect on the sheet temperature profile, but might be significant for highly transparent sheets.

5. Decreasing the period of a constant fraction of heating time has slight effect on the maximum temperature profile, but markedly increases the evenness of temperature throughout the sheet.

6. Increasing the fraction of heating time at a constant period increases the maximum temperature.

7. The results presented can be used to optimize the process of thermoforming.

From these conclusions, we find strong theoretical support for the current practice of air cooling and pulse heating temperature-sensitive sheets of semitransparent materials such as acrylics or polycarbonates.

Appendix A

Derivation of Energy Generation Term

Applying the "two-flux" method[10,13,14] to a semitransparent sheet irradiated on both sides (case 1) results in two differential equations describing the attenuation of the monochromatic energy fluxes:

$$\frac{dI}{dx} = -\alpha_i I \tag{A.1a}$$

$$\frac{dJ}{dx} = \alpha_i J \tag{A.1b}$$

whose solutions are

$$I = C_1 e^{-\alpha_i x}$$

$$J = C_2 e^{\alpha_i x}. \tag{A.2}$$

The boundary conditions for the symmetric heating model are

$$I(-L) = (1 - \rho)Q_{T\lambda} + \rho J(-L) \tag{A.3a}$$

$$J(L) = (1 - \rho)Q_{T\lambda} + \rho I(L). \tag{A.3b}$$

For nonscattering sheet, there is no difference between internal and external reflectivity.[15] Substituting the boundary conditions results in two simultaneous equations for the constants C_1 and C_2,

$$C_1 e^{\alpha_i L} = (1 - \rho)Q_{T\lambda} + \rho C_2 e^{-\alpha_i L} \tag{A.4a}$$

$$C_2 e^{\alpha_i L} = (1 - \rho)Q_{T\lambda} + \rho C_1 e^{-\alpha_i L} \tag{A.4b}$$

Evaluating the constants,

$$I = \frac{(1 - \rho)Q_{T\lambda} e^{-\alpha_i x}}{e^{\alpha_i L} - \rho e^{-\alpha_i L}}$$

$$J = \frac{(1 - \rho)Q_{T\lambda} e^{\alpha_i x}}{e^{\alpha_i L} - \rho e^{-\alpha_i L}}. \tag{A.5}$$

The monochromatic rate of energy generation within the sheet is

$$q_\lambda(x) = \alpha_i(I + J)$$

$$= \frac{\alpha_i(1 - \rho)Q_{T\lambda} \cosh \alpha_i x}{e^{\alpha_i L} - \rho e^{-\alpha_i L}}. \tag{A.6}$$

For a sheet with a discontinuous absorption curve with N continuous and finite segments, the rate of energy generation is

$$q_1(x) = \sum_{i=1}^{N} \int_{\lambda_i}^{\lambda_i + \Delta\lambda_i} \frac{\alpha_i(1 - \rho) \cosh \alpha_i x}{e^{\alpha_i L} - \rho e^{-\alpha_i L}} \, dQ_{T\lambda}. \tag{A.7}$$

Under the assumption of constant absorption coefficient over a finite wavelength and a grey body source, this equation reduces to

$$q_1(x) = \sum_{i=1}^{N} A_i \cosh \alpha_i x \tag{A.8}$$

where

$$A_i = \frac{2\alpha_i(1 - \rho)}{e^{\alpha_i L} - \rho e^{-\alpha_i L}} \int_{\lambda_i}^{\lambda_i + \Delta\lambda_i} Q_{R\lambda} d\lambda.$$

Here $Q_{R\lambda}$ can be used as long as λ_i to $\lambda_i + \Delta\lambda_i$ is interpreted as the region where α_i is finite.

For case 2, unsymmetrical heating, boundary conditions (A.3a) and (A.3b) become

$$I(-L) = (1 - \rho)I_s + \rho J(-L) \tag{A.9a}$$

and

$$J(L) = (1 - \rho)^2 \rho I(L) + \rho I(L). \tag{A.9b}$$

Again, substituting these into eqs. (A.2) and solving for C_1 and C_2, the values for I and J are determined:

$$I = \frac{(1 - \rho)Q_{T\lambda} e^{\alpha_i(L-x)}}{e^{2\alpha_i L} - \rho(\rho + (1 - \rho)^2 \rho_s) e^{-2\alpha_i L}} \tag{A.10}$$

$$J = \frac{(\rho + (1 - \rho)\rho_s)(1 - \rho)Q_{T\lambda} e^{-\alpha_i(L-x)}}{e^{2\alpha_i L} - \rho(\rho + (1 - \rho)^2 \rho_s) e^{-2\alpha_i L}}$$

and $q_2(x)$ becomes, for a grey body source,

$$q_2(x) = \sum_{i=1}^{N} D_i[(1 + \rho) \cosh \alpha_i(L - x) + (1 - \bar{\rho}) \sinh \alpha_i(L - x)] \tag{A.11}$$

where

$$I_{si} = \int_{\lambda_i}^{\lambda_i + \Delta\lambda_i} Q_{R\lambda} d\lambda; \quad \bar{\rho} = \rho + (1 - \rho)^2 \rho_s$$

and

$$D_i = \frac{\alpha_i(1 - \rho)I_{si}}{(1 + \rho\bar{\rho}) \sinh \alpha_i L + (1 - \rho\bar{\rho}) \cosh \alpha_i L}.$$

Noting that

$$e^m + \lambda e^{-m} = (1 + \lambda) \cosh m + (1 - \lambda) \sinh m$$

we can rewrite (A.11) as

$$q_2(x) = \sum_{i=1}^{N} D_i[e^{\alpha_i(L-x)} + \bar{\rho} e^{-\alpha_i(L-x)}]$$

where

$$D_i = \frac{\alpha_i(1 - \rho)I_{si}}{e^{2\alpha_i L} - \rho\bar{\rho} e^{-2\alpha_i L}}.$$

$q_3(x)$, for case 3, pulsed heating, is given by eq. (A.8) or (A.11), accordingly, wherein $Q_{R\lambda}$ is multiplied by S.

Appendix B
General Mathematical Solution

Assume a solution to eq. (1) is of the form

$$\theta(x,t) = u(x) + w(x,t). \tag{B.1}$$

Upon making this substitution into the partial differential equation and applying the specific boundary and initial conditions, a set of two coupled differential equations results, one of which represents the steady-state component and the other transient component of the time-temperature history:

$$\frac{d^2u}{dx^2} + \frac{q(x)}{k} = 0 \qquad \text{(steady-state component)} \tag{B.2}$$

subject to (case 1)

$$\left.\frac{du}{dx}\right|_{0,t} = 0; \qquad -k\left.\frac{du}{dx}\right|_{L,t} = -(1-\rho)Q_S + hu|_{L,t}$$

(case 2)

$$-k\left.\frac{du}{dx}\right|_{L,t} = hu|_{L,t}\,; \qquad -k\left.\frac{du}{dx}\right|_{-L,t} = -(1-\rho)Q_S + hu|_{-L,t}$$

(case 3 will be considered in detail below).

And

$$\frac{\partial^2 w}{\partial x^2} = \frac{1}{\kappa}\frac{\partial w}{\partial t} \qquad \text{(transient component)} \tag{B.3}$$

subject to (case 1)

$$\left.\frac{\partial w}{\partial x}\right|_{0,t} = 0; \qquad -k\left.\frac{\partial w}{\partial x}\right|_{L,t} = hw|_{L,t}$$

(case 2)

$$-k\left.\frac{\partial w}{\partial x}\right|_{L,t} = hw|_{L,t}\,; \qquad -k\left.\frac{\partial w}{\partial x}\right|_{L,t} = -(1-\rho)Q_S + hw|_{-L,t}$$

(again case 3 will be considered below).

Both solutions are coupled through the initial condition on u and w;

$$u|_x + w|_{x,0} = 0.$$

The solution to eq. (1) is thus obtained for each case by solving eq. (B.2) subject to the specific boundary conditions and definition of $q(x)$, eq. (3.1) or (3.2), solving eq. (B.3)[11] subject to its specific boundary conditions, and substituting these solutions into eq. (B.1). If the dimensionless variables and parameters defined in the text are used, the solution to eq. (1), subject to case 1 boundary conditions, is

$$\phi(\xi,t) = \sum_{n=1}^{\infty} \lambda_n e^{-\gamma_n^2\tau}\cos(\gamma_n\xi) + b - \sum_{i=1}^{N}\eta_i F_i\frac{\cosh(\Omega_i\zeta)}{\Omega_i^2} \tag{B.4}$$

where

$$a_n = \frac{\sum_{i=1}^{N}\eta_i F_i\left[\dfrac{\Omega_i\sinh\Omega_i\cos\gamma_n + \gamma_n\cosh\Omega_i\sin\gamma_n}{\Omega_i^2(\Omega_i^2+\gamma_n^2)} - \dfrac{b\sin\gamma_n}{\gamma_n}\right]}{\dfrac{1}{2}\left(1 + \dfrac{\sin\gamma_n\cos\gamma_n}{\gamma_n}\right)}$$

$$b = \frac{1}{Bi}\left\{1 + \sum_{i=1}^{N} F_i\left[\eta_i\left(\frac{\sinh\Omega_i}{\Omega_i} + \frac{Bi\cosh\Omega_i}{\Omega_i^2}\right) - 1\right]\right\}$$

$\gamma_n \tanh \gamma_n = Bi$. And the solution (again in dimensionless form) to eq. (2), subject to case 2 boundary conditions, is

$$\phi(\xi,t) = \frac{(\epsilon + \nu)\xi}{2(1 + Bi)} + \frac{(\epsilon - \nu)}{2Bi} - \sum_{i=1}^{N} \frac{\eta_i F_i}{\Omega_i^2} [e^{\Omega_i(1-\xi)} + \bar{\rho} e^{-\Omega_i(1-\xi)}] + \sum_{n=1}^{\infty} e^{-\gamma_n^2 \tau} \frac{[c_n \cos(\gamma_n \xi) + d_n \sin(\gamma_n \xi)] I_n}{(\gamma_n^2 + Bi^2) + Bi} \quad \text{(B.5)}$$

where

$$\epsilon = -Bi \sum_{i=1}^{N} \frac{\eta_i F_i}{\Omega_i^2} [e^{2\Omega_i} + \bar{\rho} e^{-2\Omega_i}] + \sum_{i=1}^{N} \frac{\eta_i F_i}{\Omega_i} (\bar{\rho} e^{-2\Omega_i} - e^{2\Omega_i}) - \left[1 - \sum_{i=1}^{N} F_i\right]$$

$$\nu = [(\bar{\rho} - 1) + (1 + \bar{\rho})Bi] \sum_{i=1}^{N} \frac{\eta_i F_i}{\Omega_i}$$

$$c_n = \sin \gamma_n [Bi + \gamma_n \cot \gamma_n]$$

$$d_n = \cos \gamma_n [Bi - \gamma_n \tan \gamma_n]$$

$$\gamma_n \tanh \gamma_n = Bi$$

$$I_n = -\frac{(\epsilon + \nu)}{(1 + Bi)} \frac{d_n}{\gamma_n^2} (\sin \gamma_n - \gamma_n \cos \gamma_n) - \frac{(\epsilon - \nu)}{Bi} \frac{c_n}{\gamma_n} \sin \gamma_n$$
$$+ c_n \sum_{i=1}^{N} \frac{\eta_i F_i}{\Omega_i^2(\Omega_i^2 + \gamma_n^2)} \{\gamma_n \sin \gamma_n [1 + \bar{\rho} + e^{2\Omega_i} + \bar{\rho} e^{-2\Omega_i}]$$
$$+ \Omega_i \cos \gamma_n [\bar{\rho} - 1 + e^{2\Omega_i} - \bar{\rho} e^{-2\Omega_i}]\}$$
$$+ d_n \sum_{i=1}^{N} \frac{\eta_i F_i}{\Omega_i^2(\Omega_i^2 + \gamma_n^2)} \{\gamma_n \cos \gamma_n [-1 - \bar{\rho} + e^{2\Omega_i} + \bar{\rho} e^{-2\Omega_i}]$$
$$+ \Omega_i \sin \gamma_n [\bar{\rho} - 1 - e^{2\Omega_i} + \bar{\rho} e^{-2\Omega_i}]\}.$$

For case 3, pulsed heating, the solution is determined by application of Duhamel's theorem[11] and the results for case 1 and case 2. For case 1, eq. (1) in dimensionless form is now written as

$$\frac{\partial \phi}{\partial \tau} = \frac{\partial^2 \phi}{\partial \xi^2} + S(\tau) \sum_{i=1}^{N} \eta_i F_i \cosh(\Omega_i \xi), \quad \text{(B.6)}$$

constraint conditions

$$\tau = 0; \quad \phi = 0$$

$$\zeta = 0; \quad \frac{\partial \phi}{\partial \xi} = 0$$

$$\zeta = 1; \quad \frac{\partial \phi}{\partial \xi} + Bi\phi - S(\tau)\left[1 - \sum_{i=1}^{N} F_i\right] = 0$$

with the dimensionless variables previously defined.

Duhamel's theorem is now applied, using the solution to case 1.[11] Let the solution to case 1 be denoted by $\phi_1(\xi,\tau)$. Further, let the nonhomogeneous terms in the governing equation and boundary condition be represented as

$$S(\tau)A(\xi)$$

where

$$A(\xi) = \sum_{i=1}^{N} \eta_i F_i \cosh(\Omega_i \xi)$$

and

$$S(\tau)g$$

where

$$g = 1 - \sum_{i=1}^{N} F_i.$$

Then, according to Duhamel's theorem, the solution to eq. (B.6) is

$$\phi(\xi,\tau) = \frac{\partial}{\partial\tau}\int_0^\tau \phi_1(\xi, \tau - \tau'; \tau')d\tau'.$$

Differentiating and applying the initial condition yields

$$\phi(\xi,\tau) = \int_0^\tau \frac{\partial}{\partial\tau}\phi_1(\xi, \tau - \tau'; \tau')d\tau'. \tag{B.7}$$

It is further specified that the nonhomogeneous terms in case 1 must be represented as $A(\xi)S(\tau')$ and $gS(\tau')$ and regarded as constant parameters in the solution of ϕ_1. Also, τ is replaced by $\tau - \tau'$. From the solution to case 1 eq. (B.4), it follows that

$$\phi_1(\xi, \tau - \tau'; \tau') = S(\tau')\left[\sum_{n=1}^{\infty} a_n e^{-\gamma_n^2(\tau-\tau')}\cos(\gamma_n\xi) + b - \sum_{i=1}^{N}\eta_i F_i \frac{\cosh(\Omega_i\xi)}{\Omega_i^2}\right] \tag{B.8}$$

where a_n and b are given below eq. (B.4).

Substituting this into eq. (B.7) and performing the indicated operations yields

$$\phi(\xi,\tau) = -\int_0^\tau s(\tau')\sum_{n=1}^{\infty} a_n\gamma_n^2 e^{-\gamma_n^2(\tau-\tau')}\cos(\gamma_n\xi)d\tau' \tag{B.9}$$

Now, if

$$S(\tau) = \begin{cases} 0, & rT < \tau < rT + T_1 \\ 1, & rT + T_1 < \tau < (r+1)T \end{cases} \qquad (r = 0,1,2,3\ldots)$$

the integrated form for eq. (B.9) becomes

$$\phi(\xi,\tau) = \sum_{n=1}^{\infty} a_n \cos(\gamma_n\xi) W_n(\tau, \gamma_n, T, T_1) \tag{B.10}$$

where

$$W_n(\tau,\gamma_n,T,T_1) = \begin{cases} e^{-\gamma_n^2\tau} - 1, & 0 < \tau \leq T_1 \\ e^{-\gamma_n^2\tau} - e^{-\gamma_n^2(\tau-T_1)}, & T_1 \leq \tau \leq T \\ e^{-\gamma_n^2\tau}\left[(e^{\gamma_n^2 T} - e^{\gamma_n^2 T_1})\sum_{s=0}^{r-1} e^{s\gamma_n^2 T} + 1 - e^{\gamma_n^2\tau}\right], & \\ \qquad rT < \tau < rT + T_1 \quad (r > 0) & \\ e^{-\gamma_n^2\tau}\left[(e^{\gamma_n^2 T} - e^{\gamma_n^2 T_1})\sum_{s=0}^{r-1} e^{s\gamma_n^2 T} + 1 - e^{\gamma_n^2(T_1+rT)}\right], & \\ \qquad rT + T_1 < \tau < (r+1)T \quad (r > 0). & \end{cases}$$

In a similar fashion, it can be shown that the pulsed heating problem for case 2 follows from Duhamel's theorem and eq. (B.5). The result is given below (unsymmetrical pulsed heating):

$$\phi(\xi,\tau) = \sum_{n=1}^{\infty} R_n(\xi) W_n(\tau, \gamma_n, T, T_1) \tag{B.11}$$

where

$$R_n(\xi) = \frac{[c_n \cos(\gamma_n \xi) + d_n \sin(\gamma_n \xi)] I_n}{(\gamma_n^2 + Bi^2) + Bi}.$$

The parameters in R_n are the same as those defined below eq. (B.5), and W_n is the same as in the previous case.

Nomenclature

A_i	coefficient, defined in text (DIT)
$A(\xi)$	function, defined in Appendix B (DIAB)
a_n	coefficient, defined in Appendix A (DIAA)
b	coefficient, DIT
Bi	Biot number, hL/k
C_1,C_2	coefficients, DIAA
c_n	coefficient, DIAB
D_i	coefficient, DIAA
d_n	coefficient, DIAB
EI	evenness coefficient, DIT
F_i	fraction of radiant energy in given wavelength band, DIT
g	function, DIAB
h	convective heat transfer coefficient, cal/cm^2 sec°K
I	monochromatic energy flux, cal/cm^2 sec, moving to right
I_s	monochromatic energy flux, cal/cm^2 sec, at left-hand surface, DIAB
J	monochromatic energy flux, cal/cm^2 sec, moving to left
k	thermal conductivity, cal/cm sec°K
L	sheet half-thickness, cm
Q_S	that fraction of radiant flux that is absorbed or reflected at the surface, cal/cm^2 sec
Q_T	that fraction of radiant flux that is transmitted into the volume of the sheet, cal/cm^2 sec
Q_R	the total radiant flux, $Q_S + Q_T$
$q(x)$	heat generation term, derived in detail in Appendix A, for all cases
$S(\tau)$	time-dependent portion of incident radiant flux, DIAB
T	material temperature, °K
T_0	ambient air temperature, °K
T_s	radiant source temperature, °K
t_p	time of period for pulsed case, sec
t_1	time of "on" portion of the pulse period, sec
t	time, sec
T	$\kappa t_p/L^2$, dimensionless time of period
T_1	$\kappa t_1/L^2$, dimensionless "on" portion of period
$u(x)$	steady-state nonhomogeneous portion of solution to eq. (1)
$w(x,t)$	transient homogeneous portion of solution to eq. (1)
W_n	function, DIAB
x	spatial coordinate, measured from center line, cm
α	absorption coefficient, cm^{-1}

γ_n eigenvalue, DIAA
ϵ coefficient, DIAB
η_{i_1},η_{i_2} dimensionless radiation parameters, DIT
θ temperature, $T - T_0$, °K
κ thermal diffusivity, cm²/sec
λ wavelength of radiation, microns
ν coefficient, DIAB
ξ dimensionless length, X/L
ρ surface reflectivity
$\bar{\rho}$ reflectivity function, DIT
ρ_s environment reflectivity (see text)
τ dimensionless time, $\kappa t/L^2$
ϕ dimensionless temperature, DIT
$\phi_1(\xi,\tau)$ solution to case 1, as used in case 3 (see Appendix B)
Ω_i radiant extinction length, $\alpha_i L$

Subscripts

i refers to wavelength band of finite absorption coefficient
λ refers to monochromatic quantity
R refers to total incident radiant flux
S refers to surface absorbed flux
T refers to transmitted flux

References

1. R. Gardon, *J. Amer. Cer. Soc.*, **39**, 278 (1956).
2. R. Gardon, *J. Amer. Cer. Soc.*, **41**, 200 (1958).
3. W. Lick, *Int. J. Heat & Mass. Trans.*, **8**, 119 (1965).
4. M. Perez and A. Baldo, *J. Franklin Inst.*, **6**, 424 (1968).
5. A. Fowle, P. Strong, D. Comstock, and C. Sox, *AIAA J.*, **7**(3), 478 (1969).
6. H. Lunka, *SPE J.*, **26**, 48 (1970).
7. F. Kreith, *Heat Transfer*, International Textbook Co., Scranton, Pa., 1966, p. 79.
8. R. C. Progelhof, J. Franey, and T. W. Haas, *J. Appl. Polym. Sci.*, **15**, 1803 (1971).
9. R. C. Progelhof, J. Quintiere, and J. L. Throne, 28th SPE ANTEC, Washington, D.C., May 7, 1971, p. 112.
10. A. Schuster, *Astrophys. J.*, **21**, 234 (1905); reprinted in D. H. Menzel, *Selected Papers on the Transfer of Radiation*, Dover, New York, 1966.
11. H. S. Carslaw and J. C. Jaeger, *Conduction of Heat in Solids*, 2nd Ed., Oxford, 1959, p. 32, 114.
12. du Pont, "Lucite" Bulletin A-63712, Wilmington, Delaware.
13. J. Klein, *Thermal Radiation of Solids*, NASA SP-55, Washington, D.C., 1965.
14. J. Richmond, *J. Res. NBS*, **67C** (3), 217 (1963).
15. R. Progelhof and J. L. Throne, *J. Appl. Optics*, **9**, 2359 (1970).
16. R. D. Cess, in *Advances in Heat Transfer*, Vol. 1, T. F. Irvine, Jr. and J. P. Hartnett, Eds., Academic Press, New York, 1964, pp. 1–52.
17. James Doyle, Research, Inc., Minneapolis, Minn., personal communication, May 18, 1972.
18. R. Jeffery, Fostoria-Fannon, Fostoria, Ohio, personal communication, June 29, 1972.
19. J. R. Hallman, J. R. Welker, and C. M. Sliepcevich, SPE Tech. Papers, **XVIII**, 283 (1972).

Received July 18, 1972